

How to build vegetation patches in hydraulic studies: a hydrodynamic-ecological perspective on a biological object

Loreta Cornacchia, Garance Lapetoule, Sofia Licci, Hugo Basquin & Sara Puijalon

To cite this article: Loreta Cornacchia, Garance Lapetoule, Sofia Licci, Hugo Basquin & Sara Puijalon (2023): How to build vegetation patches in hydraulic studies: a hydrodynamic-ecological perspective on a biological object, Journal of Ecohydraulics, DOI: [10.1080/24705357.2023.2176375](https://doi.org/10.1080/24705357.2023.2176375)

To link to this article: <https://doi.org/10.1080/24705357.2023.2176375>



© 2023 The Author(s). Published by Informa UK Limited, trading as Taylor & Francis Group



[View supplementary material](#)



Published online: 13 Feb 2023.



[Submit your article to this journal](#)



[View related articles](#)



[View Crossmark data](#)

How to build vegetation patches in hydraulic studies: a hydrodynamic-ecological perspective on a biological object

Loreta Cornacchia^{a,b}, Garance Lapetoule^a, Sofia Licci^a, Hugo Basquin^a and Sara Puijalon^a

^aUniv. Lyon, Université Claude Bernard Lyon 1, CNRS, ENTPE, UMR 5023 LEHNA, Villeurbanne, France; ^bDepartment of Water Engineering and Management, Faculty of Engineering Technology, University of Twente, Enschede, The Netherlands

ABSTRACT

Vegetation in freshwater and coastal ecosystems modifies flows, retains sediment, protects banks and shorelines from erosion. Hydraulic laboratory studies with live vegetation or artificial plant mimics, or numerical models with abstracted patches, are often used to quantify the effects of vegetation on water flow and sedimentation. However, the choice of plant and patch characteristics is often not supported by field observations of patch dimensions, density or spacing between consecutive patches. The discrepancy between plants in natural conditions and in flume experiments or numerical studies may affect the relevance of these findings for natural ecosystems. In this study, we provide guidelines for building realistic vegetation patches in hydraulic studies. We collected data on four species of fully submerged freshwater aquatic macrophytes that can grow into well-defined patches. We considered three relevant levels: individual plants (inside patches), isolated patches and multiple neighbouring patches. At the plant level, we observed significant differences in biomechanical traits (Young's modulus, flexural stiffness), resulting in stem Cauchy numbers ranging from 85.25 to 325.84, and leaf Cauchy numbers from 163.81 to 2003.97. At the patch level, we found significant relationships between patch length, width and height, showing covariation among different patch characteristics. The relationships among patch dimensions differed significantly among sampling sites for three of the four species, suggesting high intraspecific variability in patch sizes. By providing a first set of guidelines for choosing correct and ecologically relevant plant characteristics, this dataset aims to improve our understanding of the complex processes occurring inside and around submerged vegetated patches.

ARTICLE HISTORY

Received 19 April 2022
Accepted 8 January 2023

KEYWORDS



Aquatic macrophytes; hydraulic flume; numerical modelling; plant mimics; vegetation patch


1. Introduction

Vegetation modifies flow patterns, retains sediment, protects banks and shorelines from erosion and enhances nutrient retention (Haslam 1978; Franklin et al. 2008). It is important for coastal protection and the morphodynamic evolution of landscapes (Murray et al. 2008; Temmerman et al. 2013). Because of its importance for hydraulics and ecosystem functions, many studies have explored the interaction between water flow and aquatic vegetation using three main experimental approaches. First, *in situ* studies have measured flow modification induced by live vegetation (Sand-Jensen and Mebus 1996; Sukhodolova 2008; Licci et al. 2019) and compared the effects of different species (Sand-Jensen and Mebus 1996; Sand-Jensen 1998; Licci et al. 2016; Przyborowski et al. 2019). Second, these interactions have been studied in laboratory flumes with controlled conditions using real vegetation (Puijalon

et al. 2008b; Cornacchia et al. 2019b; Marin-Diaz et al. 2020). Finally, flume experiments are often carried out using artificial plant mimics (Kouwen and Unny 1973; Siniscalchi et al. 2012; Rominger and Nepf 2014; Vettori and Nikora 2018; Sukhodolov et al. 2022). Complementary to laboratory experiments, numerical modelling provides detailed information on flows over and inside the vegetation canopy, especially for processes that are difficult to measure experimentally (Marjoribanks et al. 2017; Tschisgale et al. 2021). While some studies aim for general insights on the processes and effects of vegetation using an abstracted representation of it, other studies aim to reproduce more realistic plant configurations.

The interactions between aquatic vegetation, hydrodynamics and sedimentation processes typically involve a wide range of levels of organization, from individual plants to patches (aggregation of

CONTACT Loreta Cornacchia  l.cornacchia@utwente.nl  Department of Water Engineering and Management, Faculty of Engineering Technology, University of Twente, Enschede, The Netherlands.

 Supplemental data for this article can be accessed online at <https://doi.org/10.1080/24705357.2023.2176375>.

© 2023 The Author(s). Published by Informa UK Limited, trading as Taylor & Francis Group

This is an Open Access article distributed under the terms of the Creative Commons Attribution License (<http://creativecommons.org/licenses/by/4.0/>), which permits unrestricted use, distribution, and reproduction in any medium, provided the original work is properly cited.

plants) to patch mosaics (aggregation of patches with different shapes and sizes). At the individual plant level, the modification of hydrodynamic forces and the rates of sediment deposition vary depending on the plant characteristics, such as species morphological properties and biomechanical traits (Sand-Jensen and Mebus 1996; Sand-Jensen 1998; Licci et al. 2016; Marjoribanks et al. 2019). Stem flexibility is also an important plant trait for flow-vegetation interactions: flexible vegetation has a much lower capacity to reduce hydrodynamic energy and attenuate waves than stiff vegetation, although its flexibility also leads to reduced drag (Bouma et al. 2005; Paul et al. 2012; Bouma et al. 2013). At a larger level of organization, individual plants can grow together into well-defined regions called patches (Forman 1995), which are the focus of several fluid mechanics studies because they exhibit interesting properties (Ghisalberti and Nepf 2006; Folkard 2011; Liu and Nepf 2016). Patches are composed of individual plants at high density and show sharp edges with the surrounding bare sediment (Schoelynck et al. 2018). Vegetation growth in patches can limit hydrodynamic stress on individual plants because water velocity is increased at the top of the canopy or at the edges of the patch, while individuals inside the patch are protected (Sand-Jensen and Madsen 1992; Schoelynck et al. 2013). Therefore, a patch represents a “unit element” of a canopy on which to study the interactions between hydrodynamics, vegetation and several other processes that can directly impact vegetation development (e.g. transport of nutrients, patterns of sediment erosion and deposition) (Marion et al. 2014; Folkard 2019). At this level, a higher vegetation density increases stem- and canopy-scale turbulence and sediment resuspension within the vegetation (Tinoco and Coco 2016; Yang et al. 2016). Stem-scale and patch-scale turbulence can limit the deposition of fine material downstream of a patch (Chen et al. 2012; Liu and Nepf 2016). Finally, flow deceleration within a patch occurs over an adjustment length that relates to plant morphology and patch structure (Chen et al. 2013), and a minimal patch size is required to trigger the ecosystem engineering capacity of plant patches, both in freshwater (Licci et al. 2019) and marine environments (Bouma et al. 2009). At the patch mosaic level, multiple patches create inhomogeneities in the landscape, such as gaps with recirculation zones (Kondziolka and Nepf 2014; Meire et al. 2014; De Lima et al. 2015). This kind of configuration has rarely been studied, despite many aquatic plants growing in patches that are rarely isolated.

In hydraulic laboratories, live plants are often used to reach a more realistic representation of plant-flow interactions in natural systems. Many

studies also use mimics, which are simplified but convenient for disentangling the effects of multiple plant characteristics (e.g. density and morphology; Fonseca and Cahalan (1992); Bouma et al. (2005)). Although some studies find that the behaviour of artificial mimics is different from that of real vegetation (Aberle and Järvelä 2013; Vettori and Nikora 2019), mimics offer the advantage of being more reproducible. Moreover, they prevent some of the difficulties linked to the use of real plants: flumes have to provide optimal environmental conditions (e.g. water, light availability) to keep plants alive and in good health for the duration of the experiment (Vettori and Rice 2020). Plants also continue growing during an experiment, so their morphology can change during longer-term experiments and affect the results.

While both live plants and mimics have advantages and disadvantages, for freshwater species there is a lack of data on the morphological and biomechanical characteristics of live plants and patches on which to base artificial mimics. Even in studies where live plants are used, the patch characteristics (dimensions, density) have to be chosen based on naturally observed values. In numerical models, input data are also needed to set the initial conditions and realistic parameters for the simulations. In many cases, not only the values of these parameters but also the relationships between traits or characteristics are important. There are constraints on individual plants growing in a patch, for instance, limits on the maximum height they can reach (Puijalon et al. 2008a; Puijalon et al. 2011; Marion et al. 2014) or changes in plant density with patch size (Cornacchia et al. 2022), so that not all combinations of parameter values are possible. Thus, paired data on the same species should be collected at the individual and patch levels (e.g. on single plants sampled within a patch). These findings have major implications for our ability to address scientific questions under realistic conditions and to extend the results of eco-hydraulic studies to natural conditions. There is a need to collect field data on the relationships between plant and patch traits, and on both intra- and interspecies variability that can guide the design of vegetation patches in hydraulic laboratories and that of abstracted patches in numerical studies.

This study aims to provide guidelines for designing ecologically relevant vegetation patches in hydraulic studies to achieve a more realistic representation of vegetation and advance understanding of plant-flow interactions. The study was carried out on four species of fully submerged aquatic plants (*Callitriche platycarpa* Kütz., *Groenlandia densa* (L.) Fourr., *Elodea canadensis* Michx., *Potamogeton crispus* L.) that show contrasting morphologies and

Table 1. Key characteristics of the sampling sites (with abbreviated names used in the text) along the Upper Rhône River (France). Sampling was in June for all years.

Site	Species sampled	Sampled level (year)	Coordinates	Mean water depth (m)	Mean flow velocity (m s ⁻¹)
Brégnier-Cordon (BCL)	<i>C. platycarpa</i>	Patch (2015, 2018)	45.6452 N, 5.6080 E	0.52 ± 0.18	0.21 ± 0.15
	<i>G. densa</i>	Patch (2015, 2018)			
Fléviu (FLE)	<i>C. platycarpa</i>	Patch (2015, 2018)	45.7645 N, 5.4752 E	0.61 ± 0.20	0.17 ± 0.04
	<i>Elodea</i> sp.	Patch (2015, 2018)			
Peyrieu (PEY)	<i>Elodea</i> sp.	Patch (2015, 2018)	45.6765 N, 5.6773 E	0.61 ± 0.10	0.13 ± 0.05
Serrières-de-Briord (SDB)	<i>C. platycarpa</i>	Patch (2015, 2018)	45.8153 N, 5.4269 E	0.83 ± 0.29	0.20 ± 0.07
	<i>G. densa</i>	Patch (2015, 2018)			
	<i>P. crispus</i>	Patch (2015, 2018)			
Tremurs (TRE)	<i>C. platycarpa</i>	Plant (2018, 2020)	45.6421 N, 5.6827 E	0.45 ± 0.13	0.22 ± 0.10
		Patch (2015, 2018, 2020)			
	<i>G. densa</i>	Plant (2018) Patch (2018)			
	<i>Elodea</i> sp.	Plant (2018, 2020) Patch (2018, 2020)			
	<i>P. crispus</i>	Plant (2018, 2020) Patch (2015, 2018, 2020)			

grow into patches with well-defined edges. We focussed on three levels of organization that are relevant to investigate flow-vegetation interactions: the individual plant within a patch, the patch, and the between-patch level. The individual plant level is relevant because morphological and biomechanical properties largely influence the reaction of a plant to physical forces imposed by the flow patterns, and its capacity to modify these patterns. It is also relevant for physiological processes (e.g. photosynthesis, nutrient uptake). At the patch level, flow modification is larger than that caused by single organisms: patches can modify the flow throughout the water column and at significant distances downstream, as well as modify turbulence, produce wakes, and alter sediment transport and deposition. At the between-patch level, larger-scale flow features such as interacting wakes are produced, which can increase habitat diversity, promote vegetation growth, and influence landscape development. Thus, the relevance of each of these levels of organization highlights the need for their realistic representation.

2. Materials and methods

2.1. Field sampling and study species

The four different species of freshwater macrophytes in this study were chosen because they can form well-defined patches in small freshwater streams. One of the species, *E. canadensis*, is very similar in morphology to *Elodea nuttallii* (Planch.) H. St. John, and patches often contain both species. Therefore, the plant-level and patch-level data for *Elodea* patches are labelled *Elodea* sp. and may include either one of the sampled species. Natural patches were sampled in artificial drainage channels along the Rhône River (France) that are naturally colonized by submerged vegetation (for further

description of the sampling sites, see Supporting Information Table S1 and Figure S1; Cornacchia et al. (2018); Licci et al. (2019)). During the field data collection, we focussed on three levels of organization. The following parameters were collected and paired with data on local hydrodynamic conditions (water depth and flow velocity measurements):

1. **Plant level:** plant height, dimensions of stem cross section, Young's modulus, second moment of area, flexural stiffness, Cauchy number.
2. **Patch level:** width, length, height and their allometric relationships; density; fresh and dry mass per m².
3. **Between-patch level:** species composition (% cover in the patch), minimum and maximum gap size (distance between consecutive patches), distance between patch centroids.

The characteristics of the study sites regarding the species sampled in each channel, sampling years, water depths and depth-averaged velocities are shown in Table 1. The methodology used for measuring water depth and depth-averaged velocities is described in Section 2.3.1.

2.2. Flow velocity and water depth measurements

For the plant-level measurements, we characterized the hydrodynamic conditions encountered by plants (Table 2). A vertical profile was measured 1 m upstream from the leading edge of each sampled patch, using an Acoustic Doppler Velocimeter (ADV, FlowTracker Handheld ADV, SonTek, USA). For each profile, flow velocity was measured at five vertical locations of 5%, 10%, 20%, 40% and 90% of

Table 2. Data on individual plants within patches for the four macrophyte species: average morphological and biomechanical traits [plant height (cm), dimension of stem cross-section (diameter for species with circular cross-section, major axis length for elliptical cross-sections, in mm), Young's modulus (MPa), second moment of area ($\times 10^{-13} \text{ m}^4$), flexural stiffness ($\times 10^{-5} \text{ N m}^2$)]. All traits are expressed as the mean (\pm SD) of the values for observed individuals (number of individuals indicated next to the species name).

Species	Plant height (cm)	Dimension of stem cross-section (mm)	Young's modulus (MPa)	Second moment of area ($\times 10^{-13} \text{ m}^4$)	Flexural stiffness ($\times 10^{-5} \text{ N m}^2$)	Stem Cauchy number (-)	Leaf Cauchy number (-)	Upstream flow velocity (m s^{-1})
<i>Callitriche platycarpa</i> (n = 170)	27.1 \pm 9.6	0.70 \pm 0.17	1191.45 \pm 1428.88	0.172 \pm 0.266	0.851 \pm 0.628	95.27 \pm 229.65	357.26 \pm 424.04 (n = 32)	0.13
<i>Groenlandia densa</i> (n = 10)	35.0 \pm 10.4	1.79 \pm 0.16	42.05 \pm 16.28	5.25 \pm 1.95	2.11 \pm 0.90	85.25 \pm 82.13	N/A	0.12
<i>Elodea</i> sp. (n = 105)	52.6 \pm 14.1	1.59 \pm 0.26	119.78 \pm 44.66	3.68 \pm 2.31	3.94 \pm 2.02	325.84 \pm 273.33	163.81 \pm 126.90 (n = 95)	0.19
<i>Potamogeton crispus</i> (n = 105)	51.6 \pm 20.8	2.4 \pm 0.41	66.29 \pm 48.38	53.4 \pm 478.5	3.18 \pm 1.45	297.35 \pm 417.50	2003.97 \pm 2531.63 (n = 25)	0.12

Table 3. Patch level data for the four macrophyte species in either monospecific or mixed patches: canopy length, width, rooted length, canopy height and water depth (m), as well as flow velocity measured 1 m upstream of the canopy. Values are expressed as the mean (\pm SD) across observed patches (numbers of observed patches indicated next to the species names). The sizes of mixed patches were obtained from aerial photographs, and therefore, only the canopy length and width could be measured.

Species	Canopy length (m)	Canopy width (m)	Rooted length (m)	Max. canopy height (h, m)	Water depth (H, m)	Submergence ratio (H/h)	Upstream flow velocity (m s^{-1})
<i>Callitriche platycarpa</i> (n = 38)	1.22 \pm 0.79	0.41 \pm 0.27	0.70 \pm 0.50	0.30 \pm 0.17	0.60 \pm 0.20	2.74 \pm 1.79	0.20 \pm 0.08
<i>Groenlandia densa</i> (n = 26)	1.30 \pm 0.74	0.72 \pm 0.49	1.25 \pm 0.77	0.17 \pm 0.13	0.59 \pm 0.35	4.20 \pm 2.04	0.26 \pm 0.14
<i>Elodea</i> sp. (n = 31)	1.31 \pm 0.99	0.42 \pm 0.26	1.05 \pm 1.08	0.20 \pm 0.13	0.64 \pm 0.15	4.94 \pm 3.55	0.13 \pm 0.05
<i>Potamogeton crispus</i> (n = 13)	1.11 \pm 0.49	0.47 \pm 0.56	0.58 \pm 0.64	0.20 \pm 0.11	0.62 \pm 0.30	3.66 \pm 1.96	0.28 \pm 0.07
Mixed <i>C. platycarpa</i> – <i>B. erecta</i> – <i>Elodea</i> sp. (n = 4)	3.68 \pm 1.59	1.48 \pm 0.97	–	–	–	–	–
Mixed <i>B. erecta</i> – <i>Elodea</i> sp. (n = 7)	2.83 \pm 2.48	1.45 \pm 0.78	–	–	–	–	–
Mixed <i>C. platycarpa</i> – <i>B. erecta</i> (n = 9)	2.65 \pm 1.38	1.89 \pm 1.37	–	–	–	–	–
Mixed <i>C. platycarpa</i> – <i>Elodea</i> sp. (n = 6)	1.11 \pm 0.51	0.98 \pm 0.97	–	–	–	–	–

the depth above the riverbed. Velocity was recorded over 100 s at 1 Hz.

For the patch-level measurements in 2015, the mean flow velocity (1 m upstream of the leading edge of each patch; Table 3) was measured using the ADV FlowTracker at 40% of the depth above the riverbed over 20 s at 1 Hz. At the same location, the water depth was measured with a ruler. These measurements were carried out at 31 points at site BCL, 21 points at FLE, 15 at PEY, 28 at SDB and 15 at TRE and averaged to obtain the mean water depth and mean flow velocity for each sampling site (Table 1).

2.3. Plant-level measurements

For each species, a monospecific patch of average length was selected for coupled measurements of hydrodynamics, morphological and biomechanical traits (Figure 1a).

2.3.1. Morphological traits

Ten individual plants were sampled per patch to measure maximum plant height, fresh and dry mass (leaves, roots, and stems), dimension of stem cross section, Young's modulus, second moment of area and flexural stiffness and for calculation of the

Cauchy number (Section 2.3.3). The maximum plant height (cm) was measured in the laboratory with a ruler, by laying the plant on a flat surface and stretching the plant. To measure mass (g), the plants were divided into roots, stems and leaves. The different parts were weighed to obtain fresh mass (after blotting the excess water from the plant with absorbent paper) and dry mass (measured after drying in the oven for 48 h at 60 °C). The dimension of the stem cross-section (mm) was measured using a digital calliper (± 0.02 mm) at the basal part of the stem. This dimension was the diameter for species with circular cross-sections and the length of the major axis for species with elliptical cross-sections.

2.3.2. Biomechanical traits

Biomechanical traits were measured through bending tests on 10 replicate individuals per species using a universal testing machine (Instron 5942, Canton, MA, USA). The species considered all have a caulescent growth form: the stem bears the leaves (canopy), and the bending of the stem is a key element for plant bending (movement with the flow) and canopy reconfiguration. Therefore, bending tests were carried out on the basal part of the main stem (Hamann and Puijalón 2013). However, due to the very high flexibility of the stems of the species studied, a three-point

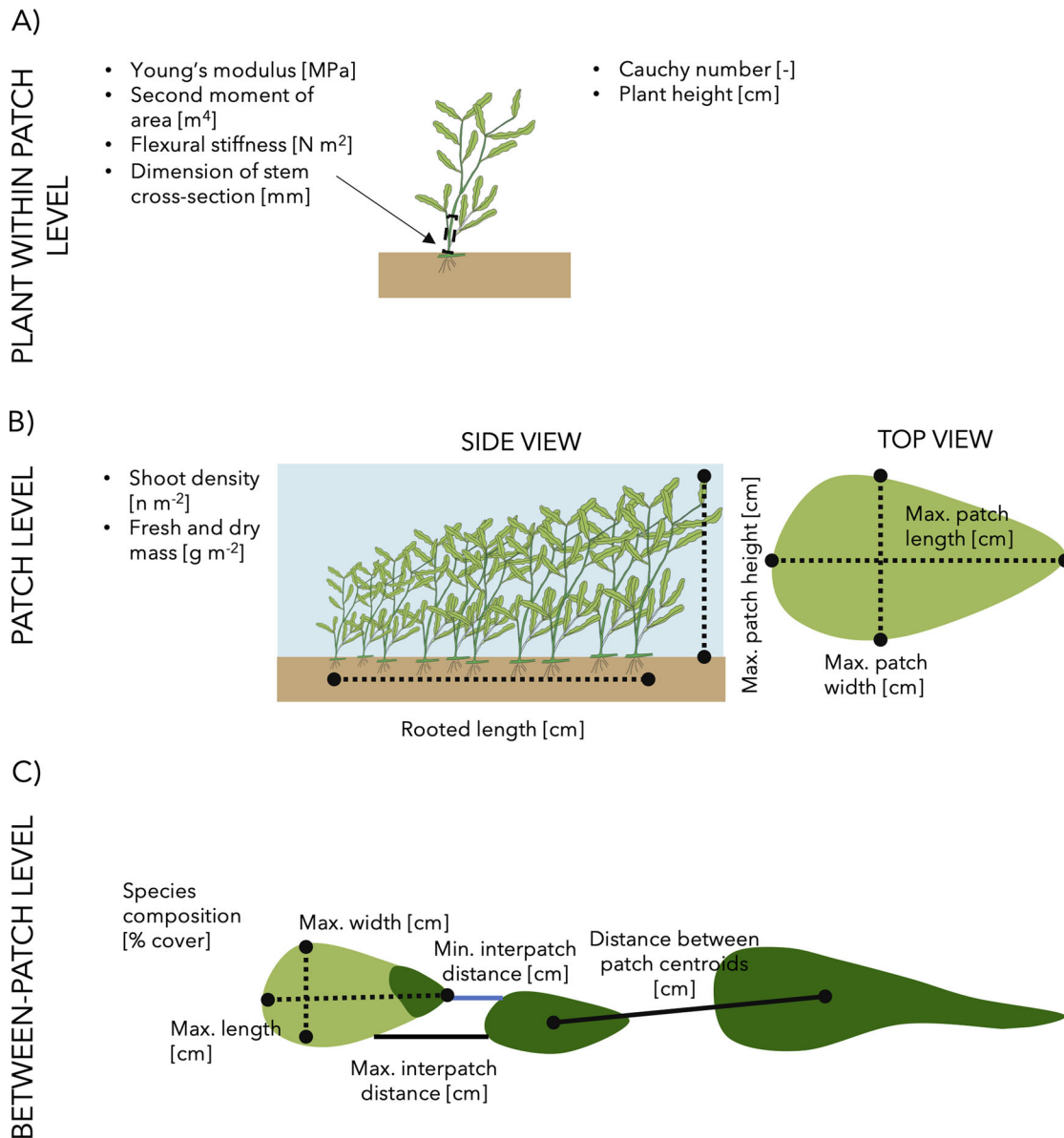


Figure 1. Overview of the measurements carried out on different aquatic macrophyte species at three different levels of organization (individual plant within patch, patch and between-patch). At level C, the different colours represent different species. The macrophyte illustration is by Dieter Tracey, Marine Botany UQ, and was sourced from the Integration and Application Network (ian.umces.edu/media-library, CC BY-SA 4.0).

bending test could not be performed on the samples because the samples tend to slip off the support bars. The samples were tested as cantilever beams using a one-fixed end bending test (Hamann and Puijalon 2013), where each stem sample (5 cm in length) was clamped horizontally at its basal end while a force was applied at the midpoint of the sample by lowering a probe at a constant rate of $10\ mm\ min^{-1}$. The following biomechanical traits were calculated:

1. The bending Young's modulus (E in MPa) quantifies the sample stiffness and is defined as the slope of a sample's stress-strain curve in the elastic deformation region.
2. The second moment of area (I in m^4) quantifies the distribution of material around the axis of bending, accounting for the effect of the cross-sectional geometry of a structure on its bending

stress. Because the stem cross-sections for *C. platycarpa*, *G. densa* and *Elodea* sp. are approximately circular, I was calculated as $I = (\pi r^4)/4$, where r is the radius of the stem cross-section (Niklas 1992). The stem cross-section of *P. crispus* is elliptical; hence, I was calculated as $I = (\pi/4)ab^3$, where a and b are the shorter and longer axes of an elliptical cross-section, respectively.

3. The flexural stiffness (EI in $N\ m^2$) was calculated by multiplying E and I and quantifies the stiffness (resistance to bending) of the stem.

2.3.3. Cauchy number

The Cauchy number is a dimensionless parameter that describes the degree of plant reconfiguration in response to flow and is the ratio between the hydrodynamic drag and the restoring force due to stiffness. In this study, the Cauchy number based on

stem dimensions was calculated as follows:

$$Ca_S = \frac{\rho U^2 dL}{EI/L^2} \quad (1)$$

where ρ is the water density (1000 kg/m³), U is the mean flow velocity (m s⁻¹), d is the dimension of the stem cross-section (m), L is the plant length (m), and EI is the flexural stiffness (N m²). Eq. 1 is similar to the calculation method applied by Luhar and Nepf (2011) to seagrass blades, but blade width is replaced by the dimension of stem cross-section because we consider species with circular or elliptical stem cross-sections. Since the leaves of aquatic plants also contribute to hydrodynamic drag, a Cauchy number based on total leaf area was also calculated for a subsample of the individuals of all species, except *G. densa*:

$$Ca_L = \frac{\rho U^2 A}{EI/L^2} \quad (2)$$

where A is the total leaf area without reconfiguration (Zhang and Nepf 2022). The total leaf area was measured on a subsample of plants by separating the individual leaves from the stems, scanning and measuring them using WinFOLIA software (Regent Instruments Inc.).

2.4. Patch-level measurements

For each species, vegetation patches were selected to cover the full range of lengths observed at the field sites, from very short (on the order of 10 cm) to very long (on the order of meters). A patch was identified as a well-defined vegetated area, clearly isolated from surrounding bare areas or from other vegetation patches. The measurements taken at this level were the patch dimensions, fresh and dry mass and shoot density per m² (Figure 1b), where a plant shoot consists of a stem and leaves. This sampling was not designed to make a link between patch dimensions and the local flow regime, but rather to look for patches of specific sizes to cover the full range of lengths observed at the field sites.

2.4.1. Patch dimensions

The general morphology of the patch was measured in terms of the maximum patch length, width, height and length of the rooted region. These measurements were taken with a tape measure. Due to the continuous movement of the plants with the current, these variables have a measurement uncertainty of a few centimetres.

Additionally, in the 2020 sampling, the field measurements of patch dimensions were also coupled with low-altitude aerial photographs on which the surface areas of patches (viewed from the

top) were measured by image analysis. The photographs were taken with a digital camera mounted on a pole at approximately 2 m height. The surface area of each patch was used to calculate the total dry mass per surface area (Section 2.3.2).

2.4.2. Patch fresh mass, dry mass and shoot density

Measurements of patch fresh and dry mass per m² were taken in June 2018 and in summer 2020. In 2018, 39 patches of different lengths were sampled (17 patches of *C. platycarpa*, 9 of *G. densa*, 10 of *Elodea* sp. and 3 of *P. crispus*). A corer with a diameter of 8 cm was used to sample the biomass in the middle of the patch. The samples were brought back to the laboratory to measure fresh mass, and dry mass was measured after drying in the oven at 60 degrees for 48 h. Based on the surface area sampled with the corer, the dry mass was expressed as total (aboveground and belowground) dry mass per unit surface area (g m⁻²).

For the 37 patches sampled in 2020 (17 patches of *C. platycarpa*, 10 of *Elodea* sp. and 10 of *P. crispus*), whole patches were collected in the field. Due to the large amount of plant material to be analysed, each patch was divided into subsamples. The fresh mass was measured for all subsamples, while the dry mass was obtained only for a subsample of the total. Based on the FM:DM ratio in the subsamples, the total dry mass for the whole patch was estimated from the total fresh biomass. Using the patch surface areas obtained from image analysis, the total patch dry mass was used to calculate total dry mass per unit surface area (g m⁻²).

Shoot density (number per m²) was also calculated for each of the four species. This was estimated by sampling 10 individuals per patch and calculating an average dry mass per plant. The total dry mass per m² was divided by the average dry mass per plant to obtain the shoot density per m².

2.5. Between-patch level measurements

To measure the gaps, or distances, between different patches (Figure 1c), a series of low-altitude aerial photographs were collected at sites PEY and FLE. At PEY, the community was composed of *Veronica anagalloides*, *Nasturtium officinale* and *Elodea* sp. In FLE, the most common species were *Callitriche platycarpa* and *Berula erecta*, with a few patches of *Myriophyllum* sp., *Elodea* sp., and *V. anagalloides*.

The photographs were taken with a digital camera mounted on a pole at approximately 2 m height. All photos were taken along a stretch of 100 m from upstream to downstream at each site, with an overlap of 80% between pictures and a 2-m ruler (with

0.1 m units) for scale in each picture. Aerial photographs were collected between May 23rd and June 14th, 2018, at times of day when the sun was at its highest point, and in the few hours before and after (between 10:00 and 14:00 h), to reduce the effect of sun glare. The pictures were mosaicked together using Autopano software, and the species were identified (together with the % cover of each species, in the case of mixed patches). After that, polygons were drawn manually to delineate each vegetation patch using ImageJ to measure the maximum patch length, width, and the minimum and maximum gap length between consecutive patches. Furthermore, the centroid of each patch polygon was identified to measure the shortest distance between centroids of adjacent patches. To limit user bias, all measurements were carried out by a single person. A comparison of the patch dimensions measured in the field and those measured from the aerial images ($n = 38$) showed that patch lengths were measured with an accuracy of 2.8%, and patch widths with an accuracy of 4.5%.

2.6. Statistical analyses

A linear mixed model, using maximum likelihood, was used to test for differences in biomechanical traits across species. This model included species as the fixed effect and individual plant as a random effect (to account for nonindependence between the individual plants sampled within the same patch). The dependent variables were Young's modulus, second moment of area and flexural stiffness.

For each species, ANCOVAs were used to test how the relationships between patch length and width, and between patch length and height, differed among sampling sites (i.e. intraspecies variability). For each species, the ANCOVA was carried out on the patch width or patch height (dependent variable), using the length as a covariate and the site as a categorical predictor. Length, site, and their interaction were included in the model at first, and non-significant interaction terms were then removed to obtain the final model. Finally, a Tukey–Kramer test was applied to investigate which slopes and intercepts differed. Two-way ANOVA was used to test the effects of sampling site and patch length on the patch dry mass per m^{-2} within each species. For all traits and characteristics, we also tested for any significant differences between sampling years (further described in Supporting Information, Appendix S1). All statistical analyses were performed in R 4.0.3 (R Core Team 2020).

The ANCOVA and ANOVA were conducted on independently collected samples after testing for normality and homoscedasticity of the data

(Shapiro-Wilk and Brown-Forsythe tests). In addition to the above assumptions, the ANCOVA was conducted only if, for each site category, there was a significant linear relationship between the dependent variable and the covariate, and if the ranges of the dependent variable overlapped between the different categories. Therefore, ANCOVA was not performed on *P. crispus* as the relationship between the covariate and dependent variable was significant for only one site, and on *Elodea* sp. for the relationship between patch length and height.

3. Results

3.1. Plant-level data

Plant-level data for the four studied species are presented in Table 2. Across all species, plant height ranged on average from 27.1 cm (*C. platycarpa*) to 56.2 cm (*Elodea* sp.), while the stem cross-section dimension ranged from 0.70 mm (diameter for *C. platycarpa*) to 2.4 mm (major axis length for *P. crispus*). The second moment of area was highly variable among species, ranging across multiple orders of magnitude (10^{-12} to 10^{-14} m^4). Flexural stiffness varied between 10^{-5} and 10^{-6} N m^2 , while the Young's modulus ranged from 42.05 to 1191.45 MPa. Based on these parameters, the stem Cauchy number Ca_S (Table 2) ranged from 85.25 (for *G. densa*) to 325.84 (for *Elodea* sp.). The Cauchy number based on total leaf area Ca_L was 4 to 7 times larger than Ca_S for two of the species (*C. platycarpa* and *P. crispus*), indicating the contribution of leaves to the hydrodynamic drag. However, for *Elodea* sp., Ca_L was 50% smaller than Ca_S .

We found significant differences in the biomechanical traits of the investigated species in terms of Young's modulus ($F_{3,36} = 19.8$, $p < 0.001$) and flexural stiffness ($F_{3,36} = 29.7$, $p < 0.001$). The Young's modulus of *C. platycarpa* was significantly higher than that of *Elodea* sp. and *P. crispus* (Tukey's HSD, $p < 0.001$ for both pairwise comparisons) but not significantly different from that of *G. densa* (Tukey's HSD, $p = 0.07$). *C. platycarpa* had the highest flexibility, with a significantly lower flexural stiffness than that of *Elodea* sp. and *P. crispus* (Tukey's HSD, $p < 0.001$ for both pairwise comparisons) but not compared to *G. densa* (Tukey's HSD, $p = 0.53$). Between the sampling years (2018 and 2020), we found significant differences in Young's modulus for *P. crispus*, in second moment of area for *C. platycarpa* and *P. crispus*, and in flexural stiffness for *C. platycarpa* and *Elodea* sp. (Supporting Information Table S2). Moreover, we found significant differences in the dimension of the stem cross-section for *C. platycarpa* and *Elodea* sp.

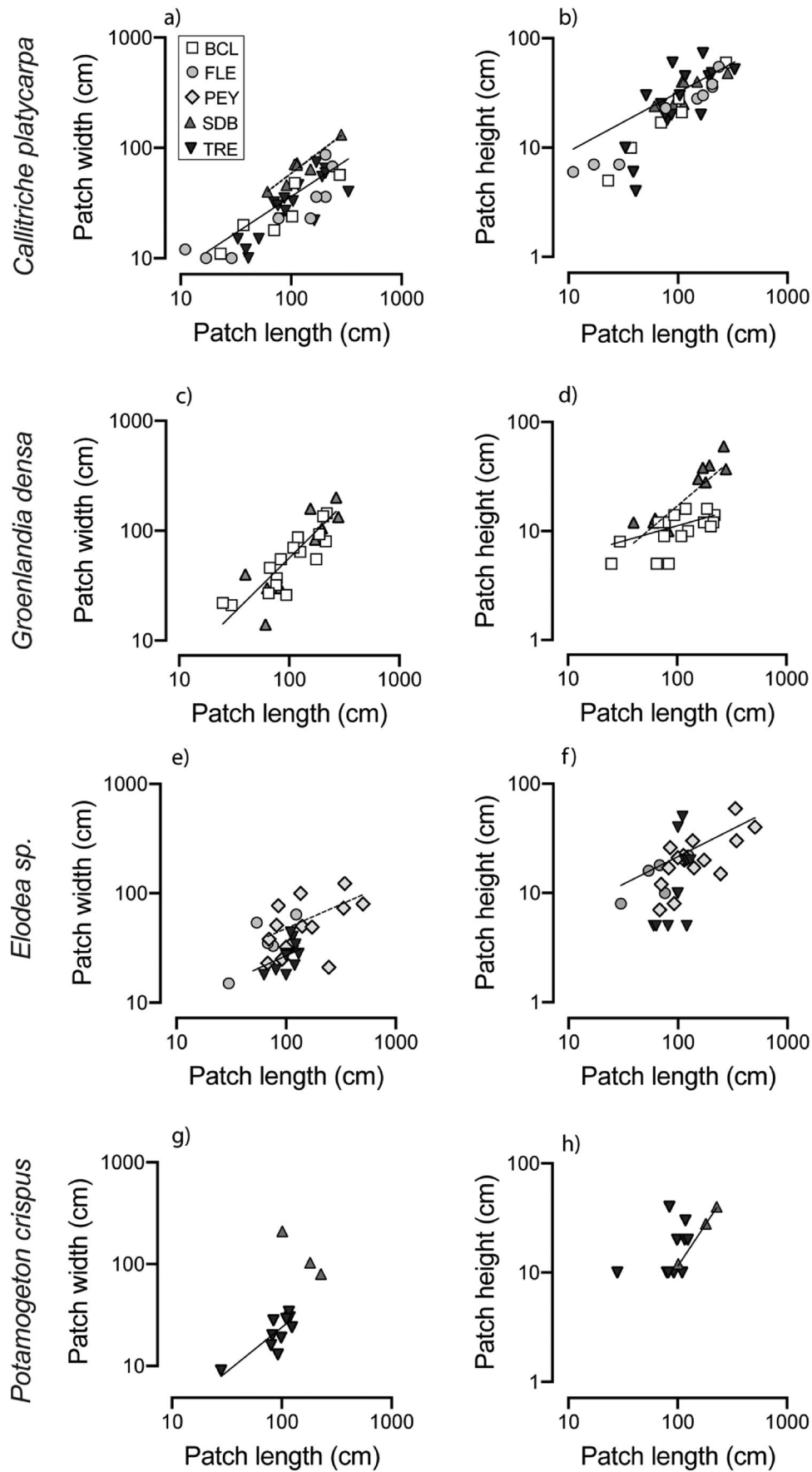


Figure 2. Allometric relationship between patch length, width and height for *Callitriche platycarpa*, *Groenlandia densa*, *Elodea sp.* and *Potamogeton crispus*. Different symbols indicate the sampling sites. Different regression lines are plotted if significant differences in the relationship were found among sites. In (a), the dashed regression line refers to site SDB and the solid line is for all other sites. In (b) and (c), one regression line refers to all sites. In (d), dashed line refers to site SDB, solid line to site BCL. In (e), dashed line is for site PEY, solid line for site TRE. In (f), the regression line refers to site PEY; in (g), to site TRE; in (h), to site SDB. Statistical descriptions of the relations are provided in [Table 5](#).

Table 4. Relationships among the patch width, patch height and patch length, sampling site and interactions between patch length and site per species (ANCOVA tests). Nonsignificant interaction terms that were successively dropped are indicated in italics (F and p value correspond to the model with higher-order interaction where the term is present).

Dependent variable: patch width			
	<i>C. platycarpa</i>	<i>G. densa</i>	<i>Elodea</i> sp.
Length	$F_{1,33} = 52.92, p < 0.001$	$F_{1,23} = 67.37, p < 0.001$	$F_{1,23} = 16.21, p < 0.001$
Site	$F_{3,33} = 9.83, p < 0.001$	$F_{1,23} = 0.59, p = 0.448$	$F_{1,23} = 4.28, p = 0.05$
Length × Site	$F_{3,30} = 2.38, p = 0.09$	$F_{1,22} = 0.62, p = 0.44$	$F_{1,22} = 0.39, p = 0.5$
Dependent variable: patch height			
	<i>C. platycarpa</i>	<i>G. densa</i>	
Length	$F_{1,33} = 46.9, p < 0.001$	$F_{1,22} = 80.93, p < 0.001$	
Site	$F_{3,33} = 0.88, p = 0.46$	$F_{1,22} = 42.76, p < 0.001$	
Length × Site	$F_{3,30} = 0.51, p = 0.67$	$F_{1,22} = 23.19, p < 0.001$	

Table 5. Regression lines of the allometric relationships between patch length, width, and height (presented in Figure 2). The independent variable (x) is patch length.

Species	Dependent variable (y)	
	Patch width	Patch height
<i>C. platycarpa</i>	$y = 0.218x + 42.18$ (site SDB) $y = 0.218x + 7.57$ (other sites)	$y = 0.16x + 7.95$ (all sites)
<i>G. densa</i>	$y = 0.56x + 0.17$ (all sites)	$y = 0.138x + 2.23$ (site SDB) $y = 0.033x + 6.7$ (site BCL)
<i>Elodea</i> sp.	$y = 0.13x + 31.38$ (site PEY) $y = 0.13x + 13.03$ (site TRE)	$y = 0.078x + 9.36$ (site PEY)
<i>P. crispus</i>	$y = 0.218x + 1.8$ (site TRE)	$y = 0.218x - 10.44$ (site SDB)

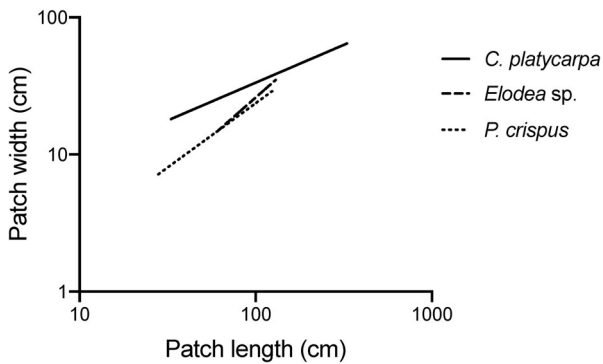


Figure 3. Summary view of the differences in the relationship between patch length and patch width for species living in the same environmental conditions (site TRE), indicating differences in the growth modes of each species.

3.2. Patch dimensions

The mean patch sizes for all species are shown in Table 3. The longest observed patches were of *Elodea* sp. (5.0 m), followed by *C. platycarpa* (3.3 m) and *G. densa* (2.8 m). The ratio of patch width to length appeared to decline for longer patches of *C. platycarpa* and *Elodea* sp., possibly due to water flow diversion around longer patches, which limits their expansion in width.

The relations between patch dimensions (that between patch length and width and that between patch length and height) differed by sampling site in some cases, suggesting a degree of intraspecies variability (Figure 2). For *C. platycarpa* and *Elodea* sp., the effect of the interaction between length and site on patch width was not significant, whereas the effects of both length and site were significant (Table 4). These results indicate that for each

species, the slopes of the relationships between length and width did not significantly differ among sites. For these two species, only the intercepts of the relationships between length and width differed among sites, with the patches sampled at site SDB being wider for a given length than those at the other sites for *C. platycarpa*, and the patches sampled at site PEY being wider for a given length than those at site TRE for *Elodea* sp. For *G. densa*, the effects of both the interaction between length and site and the site were not significant (Table 4), indicating that the relationship between length and width did not differ among the sampling sites.

In the relationship between patch length and height of *C. platycarpa*, the effects of both the interaction between length and site and the site were not significant (Table 4), indicating that the relationship between length and height did not differ among the sampling sites. For *G. densa*, the interaction between length and site was significant (Table 4), indicating that the relationship between height and length varied in slope among sampling sites (smaller slope for site BCL than for site SDB). In the range of patch lengths sampled, for a given length, the patches had lower heights at site BCL than at site SDB. A statistical description of all the relationships is provided in Table 5. We found no significant differences in the relationships between patch dimensions among sampling years, except for that between patch length and width of *Elodea* sp. (Supporting Information Table S3).

To illustrate the extent to which species can grow differently under similar environmental conditions, we considered the allometric relationships at the TRE site, where three of the four species are found

Table 6. Patch fresh and dry mass (aboveground and belowground) per m^2 and shoot density (number per m^2) for different macrophyte species. Shoot density was estimated based on the average dry mass of 10 shoots per species and patch total dry mass. Values are expressed as the mean (\pm SD) across sampled patches (number of patches sampled are indicated next to the species names; the fresh and dry mass were measured on the same patches).

Species	Fresh Mass ($g\ m^{-2}$)	Dry Mass ($g\ m^{-2}$)	Shoot density ($n\ m^{-2}$)
<i>Callitriche platycarpa</i>	4062.1 ± 6124.8 ($n = 33$)	228.9 ± 263.4	4468 ± 4826 ($n = 16$)
<i>Groenlandia densa</i>	2458.5 ± 674.8 ($n = 9$)	267.2 ± 69.9	1591 ± 416 ($n = 9$)
<i>Elodea</i> sp.	1819.1 ± 1268.0 ($n = 19$)	155.7 ± 100.2	364 ± 236 ($n = 10$)
<i>Potamogeton crispus</i>	1159.7 ± 1585.3 ($n = 13$)	133.8 ± 181.8	238 ± 149 ($n = 10$)

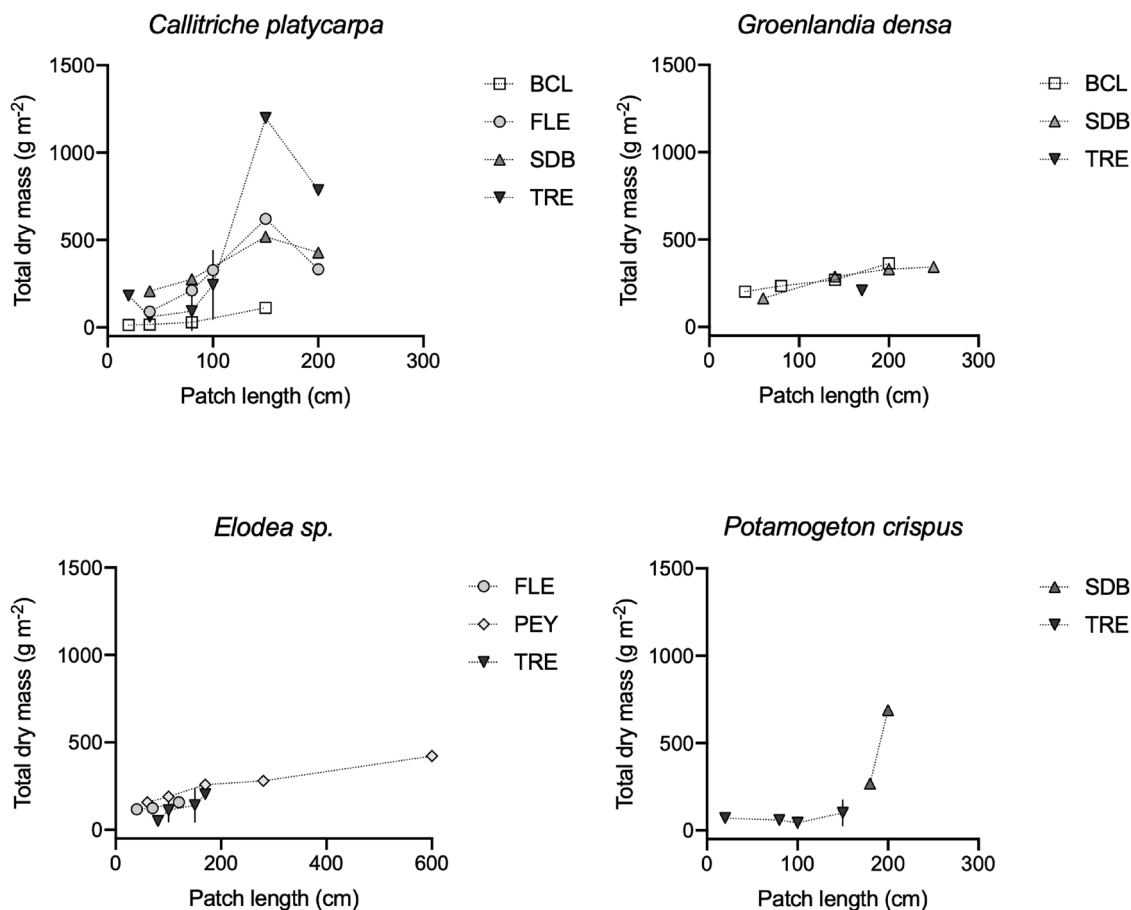


Figure 4. Total (aboveground and belowground) dry mass per unit surface area ($g\ m^{-2}$) of vegetation patches of increasing length sampled at different sites. Error bars, when present, represent the SD among replicate patches in the same length category. Note the different x-axis range in *Elodea* sp. Dotted lines connect the data points for visualization.

(Figure 3). These differences in the relationship between patch length and width can be related to water flow diversion and acceleration along the sides of a patch, which limits its expansion in width. The intensity and scale of this negative feedback likely differs among species and could determine the size of the pattern, as found in other ecosystems (Rietkerk and van de Koppel 2008).

3.3. Patch fresh mass, dry mass and shoot density

Values of total (aboveground and belowground) patch fresh and dry mass per unit surface area are presented in Table 6. The total dry mass per unit

surface area tended to increase with patch length for all species (Figure 4). However, in the case of *C. platycarpa*, it reached a maximum in patches of 1.5 m length across different sites and declined again for the largest patches (> 2 m). For this species, total dry mass was significantly higher in intermediate patches (1.0–1.5 m length class) than in shorter patches between 0.2 and 0.8 m in length (two-way ANOVA, $F_{5,14} = 3.68$, $p = 0.02$). No significant differences were found among the sampling sites. We found no significant differences in total dry mass between sampling years (2018 and 2020), except for *C. platycarpa* (Supporting Information Table S2).

For *P. crispus*, the total patch dry mass ($g\ m^{-2}$) significantly differed among sites (two-way ANOVA,

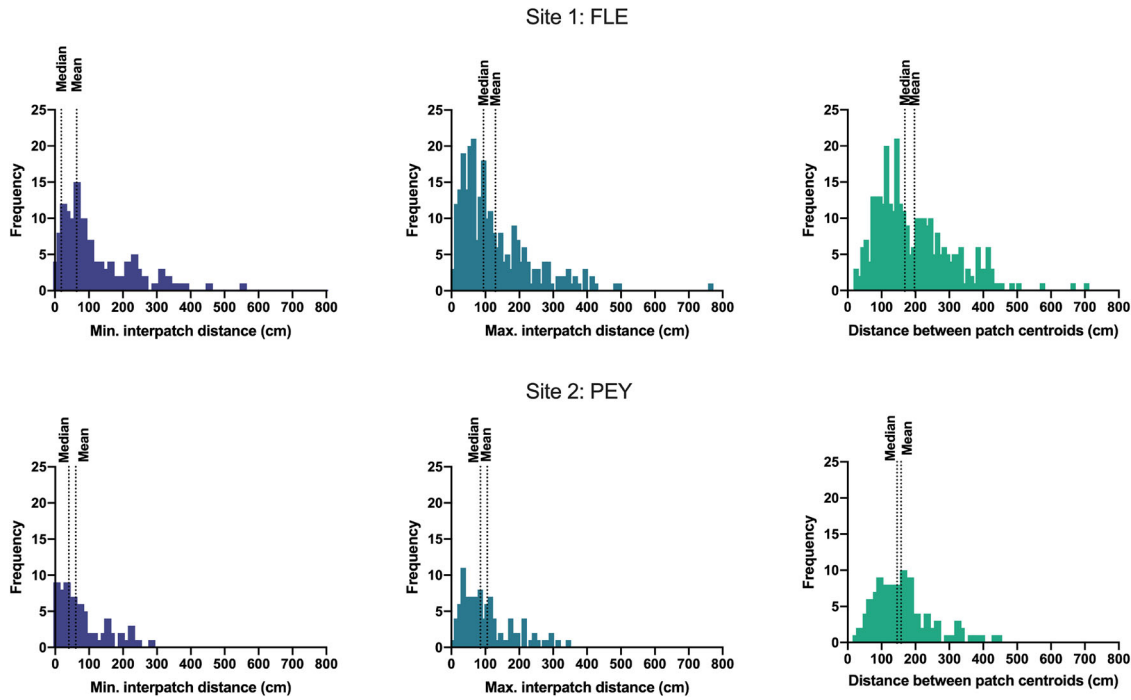


Figure 5. Frequency distributions of minimum and maximum interpatch distances and distances between patch centroids for the sites of FLE (top panels) and PEY (bottom panels).

$F_{1,8} = 20.63$, $p < 0.01$), with patches at the TRE site showing significantly higher biomass than those at the SDB site (post-hoc Tukey test, $p < 0.01$). For *Elodea* sp., the patches sampled at site PEY had significantly higher dry mass than those sampled at site TRE (post-hoc Tukey test, $p < 0.05$). For *G. densa*, no significant difference was observed among patches sampled at different sites (one-way ANOVA, $F_{2,6} = 0.36$, $p = 0.7$).

The shoot density, reported in Table 6, ranged from an average of 238 shoots per m^2 within patches of *P. crispus* up to 4468 shoots per m^2 in *C. platycarpa*.

3.4. Species composition at the between-patch level

At site PEY, all patches ($n = 100$) were monospecific: 68% were made up of *V. anagalloides*, 27% of *N. officinale*, 2% of *Elodea* sp. For the remaining 3% of the patches, the species could not be clearly identified from the images. At site FLE, the species composition in the patches ($n = 209$) was more variable, with 83% of patches monospecific and 17% mixed. Within the monospecific patches, 69% were composed of *C. platycarpa*, 24% of *B. erecta*, 3% of *Myriophyllum* sp., 2% of *Elodea* sp. and 2% of *V. anagalloides*. Among the mixed patches, 26% were a mixture of *C. platycarpa*, *Elodea* sp. and *B. erecta*; 26% were *B. erecta* and *Elodea* sp.; 26% were *C. platycarpa* and *B. erecta*; and the remaining 22% were *C. platycarpa* and *Elodea* sp. The patch sizes of the mixed patches are reported in Table 3 (note that the number of mixed patches can

be lower than indicated by the percentages, because the size was not measured if the patch was not entirely captured in the aerial picture).

3.5. Interpatch distances

The minimum and maximum interpatch distances had comparable distributions at sites FLE and PEY, with both sites showing positively skewed distributions (Figure 5). In FLE, the minimum distance ranged between 0 cm (no visible gap between patches) and 554.0 cm, with a mean of 63.8 and a median of 18.5 cm. The maximum distance ranged between 4 and 770 cm (mean of 129.2 and median of 94.0 cm). At PEY, the distances were generally lower than those at FLE, and minimum distances varied between 0 and 286 cm (mean of 60.5 and median of 40 cm). The maximum distances varied between 10 and 341 cm (mean of 105.5 and median of 85.5 cm).

When analysing the distances between patch centroids (Figure 5), we found a mean distance of 197 cm (median 168.5 cm) at FLE. The centroid distances varied between 23 cm and 708 cm. Among the observed distances ($n = 314$), 75% were oriented in the main direction of flow, but they were oriented in a different direction in 25% of the cases, which indicated that staggered patch distributions were observed.

Mean distances between patch centroids were also comparable at PEY, where the mean value was 157.5 cm (median 145 cm). The observed range of

distances was, however, more limited compared to that at the previous site, ranging between 25 and 441 cm. Among the observed distances at this site ($n = 126$), slightly over half of the patch pairs (51%) were oriented in the main flow direction, while 49% were oriented in other directions. This indicates that patches commonly grow adjacent to each other and in complex arrangements.

4. Discussion

The present investigation aims to provide realistic vegetation parameters for ecohydraulic laboratory and numerical studies that focus on the vegetation patch as the main study unit. The parameters are provided for four different species of aquatic macrophytes at three relevant levels of organization for hydraulic studies: individual plants (inside patches), single vegetation patches and multiple neighbouring patches. We found significant relationships between patch length, width and height for the species considered (consistent with the results of Sand-Jensen and Madsen (1992) for *Callitriche cophocarpa*), except for the relationship between length and width of *P. crispus*. The relationships between patch dimensions differed significantly among sampling sites for three of the four species, suggesting a high intraspecies variability in patch size. This suggests that different species respond differently to local conditions, either because of intraspecific variability or due to phenotypic plasticity (with certain species showing higher levels of plasticity than others). Since all these cases exist and all are possible in nature, providing parameter ranges is relevant information for studies that are better suited to focus on a range of values (or minimum and maximum values), rather than on a single value. Significant differences in biomechanical traits (Young's modulus and flexural stiffness) were also observed, resulting in stem Cauchy numbers ranging from 85.25 to 325.84, and leaf Cauchy numbers between 163.81 and 2003.97. Depending on the species, shoot density varied from hundreds to a few thousand individuals per square metre. Distances between patches (gap sizes) were on average 1.5 m and although the range of observed values was quite broad, the mean and median gap sizes were comparable among the study sites. The average distance between patch centroids was also approximately 1.5 m. These data provide useful information for constructing more realistic vegetation patches in laboratory flume studies and can be equally important for modelling studies by providing a clear set of cases and initial conditions for model simulations.

The results of the biomechanical tests are comparable to the results found by Łoboda et al. (2018a,

2018b) on two of the same aquatic plant species. The bending Young's modulus was in the same order of magnitude and similar range of value as in our measurements (38.96 ± 42.60 MPa for *P. crispus* and 95.32 ± 51.59 MPa for *E. canadensis* sampled at the same time of the year). The values of second moment of area ($(8.61 \pm 5.7) \times 10^{-13}$ m⁴ for *P. crispus* and $(0.8 \pm 0.3) \times 10^{-13}$ m⁴ for *E. canadensis*) and flexural stiffness ($(2.6 \pm 2.6) \times 10^{-5}$ N m² for *P. crispus* and $(0.6 \pm 0.3) \times 10^{-5}$ N m² for *E. canadensis*) are also comparable to our study. The small differences observed may be related to the environmental conditions in the different sites.

The stem Cauchy number (Ca_S) calculated based on the data in this study was lower than that previously reported for very flexible vegetation, although it falls within the estimated range of $Ca \approx 10$ to 40,000 (for a typical velocity range of $U = 5\text{--}50$ cm s⁻¹) (Luhar and Nepf 2011). However, leaves have a strong impact on hydrodynamic drag and contribute to increase the Cauchy number: the Cauchy number based on total leaf area (Ca_L) was 4 to 7 times larger than Ca_S for two of the species (*C. platycarpa* and *P. crispus*). *Elodea* sp. was the only species where Ca_L was smaller than Ca_S but the inclusion of leaves would still contribute to increase the total Cauchy number by 50%. Considering that longer leaves and stems would increase the Cauchy number, the discrepancy may also partly arise because plants can vary greatly in length, depending on the conditions: plant length is generally higher in standing water than in running water, and there are constraints on plant length depending on patch size, as further discussed below.

4.1. Constraints on growth of plants into patches: relevance of paired data per species

A relevant aspect of this study is to provide coupled data on individual plants growing inside patches, which is crucial because there are relationships between parameters at different levels. Within a single vegetation patch, differences in plant height are found between the front and rear of the patch: plants located at the front are shorter due to the high flow stress, while plants located in the downstream portion are more sheltered and can grow longer (Gessner 1955; Cornacchia et al. 2016). Both hydrodynamic conditions and patch formation impose constraints on the size (length) of a plant. Regarding hydrodynamic conditions, size reduction has frequently been observed in single isolated plants in running systems (Puijalon and Bornette 2004; Puijalon et al. 2008b). However, the regular and compact shape of a patch is also determined by hydrodynamic constraints (constraining length of a

plant depending on its location in a patch), which also implies that a plant cannot grow long in a small patch. Therefore, the characteristics measured on a plant growing in standing conditions cannot be applied to running conditions. Our findings may inspire future research by raising the hypothesis that isolated plants are not under the same constraints as plants growing within a patch. In that case, plant and patch characteristics would need to be based as much as possible on paired data collected on a single species at both the individual and patch levels.

Our patch sampling strategy did not allow us to make a link between patch dimensions and the local flow regime. Regardless of the sampling strategy, relating patch dimensions to the local hydrodynamic conditions is challenging without a measure of patch growth rates: a patch could be long because it is growing fast in slow flow conditions, or it could be long because it has grown slowly over many years in fast flow conditions. The fact that the growth rate varies according to the flow conditions leads to this disconnection to the patch traits, so that patch age is not necessarily related to its size. Future studies are needed to follow patch growth over time to investigate how flow velocity affects patch dimensions.

To show the importance of coupled data and the relationship between different parameters, we illustrate an example of the potential errors that can occur when paired data are disregarded. In this study, the leaf Cauchy number calculated using paired data (i.e. data per species) varied between 163.81 and 2003.97. If paired data were not considered and the most extreme (minimum and maximum) values across all species were used for each variable needed to calculate the Cauchy number, the results would be different: the leaf Cauchy number would be 31.24 when the lowest values among all species are used, and it would be 5948.88 when all the highest values are used. This example illustrates the consequences of respecting the paired data per species as opposed to using a value observed for any of the species. While the covariation between characteristics might appear to increase sampling efforts as there is a need to use paired data, it may also be a way to reduce sampling effort by using proxies. The statistical relationships presented in this study between patch dimensions are one example of how sampling can be reduced, for instance by obtaining all required patch dimensions from aerial photographs.

4.2. Directions for future research on flow-vegetation interactions

The findings from this work point to vegetation properties that have thus far been overlooked in the

literature and provide useful recommendations for future research directions. For future studies on flow-vegetation interactions at the between-patch level and with the objective of exploring the role of patch configurations, we emphasize that 25 to 50% of the observed patch pairs were not oriented in the main direction of flow. This is somewhat counterintuitive considering the presence of flow acceleration and negative feedbacks next to the patches but is consistent with the findings of Cornacchia et al. (2019a), who showed that patch staggering is frequent. These data suggest that adjacent patches or more complex distributions are also quite common, as already explored in studies on vegetation tussocks in salt marshes (Vandenbruwaene et al. 2011; Meire et al. 2014). We also highlight that while monospecific patches were prevalent at one of the field sites, the other site showed a 20% occurrence of multispecies (“mixed”) patches. The study of mixed patches is thus far a largely overlooked aspect of the complexity of flow-vegetation interactions (Schoelynck et al. 2018), but due to their common occurrence in the field, we provide an indication of their sizes and species composition, and we suggest that it would be an interesting direction for future studies.

5. Conclusions

This study aims to provide data to build vegetation patches in ecohydraulic studies. Four patch-forming species of submerged aquatic macrophytes were considered, and their characteristics were studied at three levels relevant for flume and modelling studies: individual plants (inside patches), single vegetation patches and multiple patches. The key findings include the following:

1. The results show that different plant characteristics covary in natural patches, as shown by the relationships between patch length, width, and height and by the changes in dry mass with patch size. The covariation between different patch characteristics should be considered when building mimics and planning experimental conditions because not all combinations of parameter values might occur in nature.
2. Vegetation species differ from each other for “sets” of characteristics, rather than single properties: a challenge for future ecohydraulics studies will be to separate the effect of each of these characteristics on hydrodynamic and sedimentation processes. We stress the need for more studies on real patches, complemented by modelling approaches, to make progress in this direction.

Funding

The work was funded by the ANR-DFG 2016 project ESCaFlex ('Experiments and simulations for the study of submerged aquatic canopies consisting of long flexible blades', ANR-16-CE92-0020) and by the Research Executive Agency, through the Seventh Framework Programme of the European Union, Support for Training and Career Development of Researchers (Marie Curie - FP7-PEOPLE-2012-ITN), which funded the Initial Training Network (ITN) HYTECH "Hydrodynamic Transport in Ecologically Critical Heterogeneous Interfaces," N.316546. We acknowledge Baptiste Thevenet, Celine Lott, Félix Vallier, Christelle Boisselet and Sophie Poussineau for their help in field sampling and data collection. We thank Nicolas Rivière, Delphine Doppler and J. John Soundar Jerome for valuable discussions on the Cauchy number. We thank the Compagnie Nationale du Rhône (CNR) for access to field sites. This study was conducted under the aegis of the "Zone Atelier Bassin du Rhône" (ZABR, LT SER France) and of the École Universitaire de Recherche H2O'Lyon (ANR-17-EURE-0018). We thank the Editor, the Associate Editor and the anonymous reviewers for their valuable comments that have improved the quality of our manuscript.

Data availability statement

Data presented in this manuscript are available at the 4TU.Research Data repository (Cornacchia et al. 2023).

Disclosure statement

No conflict of interest has been reported by the authors.

References

- Aberle J, Järvelä J. 2013. Flow resistance of emergent rigid and flexible floodplain vegetation. *J Hydra Res.* 51(1): 33–45.
- Bouma T, De Vries M, Low E, Peralta G, Tánzos I, van de Koppel J, Herman PMJ. 2005. Trade-offs related to ecosystem engineering: a case study on stiffness of emerging macrophytes. *Ecology.* 86(8):2187–2199.
- Bouma T, Friedrichs M, Van Wesenbeeck B, Temmerman S, Graf G, Herman P. 2009. Density-dependent linkage of scale-dependent feedbacks: a flume study on the intertidal macrophyte *Spartina anglica*. *Oikos.* 118(2): 260–268.
- Bouma TJ, Temmerman S, van Duren LA, Martini E, Vandenbruwaene W, Callaghan DP, Balke T, Biermans G, Klaassen PC, van Steeg P, et al. 2013. Organism traits determine the strength of scale-dependent biogeomorphic feedbacks: a flume study on three intertidal plant species. *Geomorphology.* 180–181:57–65.
- Chen Z, Jiang C, Nepf H. 2013. Flow adjustment at the leading edge of a submerged aquatic canopy. *Water Resour Res.* 49(9):5537–5551.
- Chen Z, Ortiz A, Zong L, Nepf H. 2012. The wake structure behind a porous obstruction and its implications for deposition near a finite patch of emergent vegetation. *Water Resour Res.* 48(9):1–12.
- Cornacchia L, Folkard A, Davies G, Grabowski RC, Koppel J, Wal D, Wharton G, Puijalon S, Bouma TJ. 2019a. Plants face the flow in V formation: a study of plant patch alignment in streams. *Limnol Oceanogr.* 64(3):1087–1102.
- Cornacchia L, Licci S, Nepf H, Folkard A, Wal D, Koppel J, Puijalon S, Bouma TJ. 2019b. Turbulence-mediated facilitation of resource uptake in patchy stream macrophytes. *Limnol Oceanogr.* 64(2):714–727.
- Cornacchia L, Licci S, Van De Koppel J, Van Der Wal D, Wharton G, Puijalon S, Bouma TJ. 2016. Flow velocity and morphology of a submerged patch of the aquatic species *Veronica anagallis-aquatica* L. Hydrodynamic and mass transport at freshwater aquatic interfaces. Cham: Springer; p. 141–152.
- Cornacchia L, Riviere N, Soundar Jerome JJ, Doppler D, Vallier F, Puijalon S. 2022. Flow and wake length downstream of live submerged vegetation patches: how do different species and patch configurations create sheltering in stressful habitats? *Water Resour Res.* 58(3):1–21.
- Cornacchia L, van de Koppel J, van der Wal D, Wharton G, Puijalon S, Bouma TJ. 2018. Landscapes of facilitation: how self-organized patchiness of aquatic macrophytes promotes diversity in streams. *Ecology.* 99(4): 832–847.
- Cornacchia L, Lapetoule G, Licci S, Basquin H, Puijalon S. 2023. Data underlying the publication: how to build vegetation patches in hydraulic studies: a hydrodynamic-ecological perspective on a biological object [Data Set]. 4TU.ResearchData. <https://doi.org/10.4121/21786434>
- De Lima PH, Janzen JG, Nepf HM. 2015. Flow patterns around two neighboring patches of emergent vegetation and possible implications for deposition and vegetation growth. *Environ Fluid Mech.* 15(4):881–898.
- Folkard AM. 2011. Flow regimes in gaps within stands of flexible vegetation: laboratory flume simulations. *Environ Fluid Mech.* 11(3):289–306.
- Folkard AM. 2019. Biophysical interactions in fragmented marine canopies: fundamental processes, consequences, and upscaling. *Front Mar Sci.* 6:279.
- Fonseca MS, Cahalan JA. 1992. A preliminary evaluation of wave attenuation by four species of seagrass. *Estuarine Coastal Shelf Sci.* 35(6):565–576.
- Forman RT. 1995. Some general principles of landscape and regional ecology. *Landscape Ecol.* 10(3):133–142.
- Franklin P, Dunbar M, Whitehead P. 2008. Flow controls on lowland river macrophytes: a review. *Sci Total Environ.* 400(1–3):369–378.
- Gessner F. 1955. *Hydrobotanik, Die Physiologischen Grundlagen der Pflanzenverbreitung in Wasser.* I. Berlin: Energiehaushalt. VEB Deutscher Verlag der Wissenschaften.
- Ghisalberti M, Nepf H. 2006. The structure of the shear layer in flows over rigid and flexible canopies. *Environ Fluid Mech.* 6(3):277–301.
- Hamann E, Puijalon S. 2013. Biomechanical responses of aquatic plants to aerial conditions. *Ann Bot.* 112(9): 1869–1878.
- Haslam SM. 1978. *River plants: The macrophytic vegetation of watercourses.* Cambridge University Press; p. 396.
- Kondziolka JM, Nepf HM. 2014. Vegetation wakes and wake interaction shaping aquatic landscape evolution. *Limnol Oceanogr Fluids Environ.* 4(1):106–119.
- Kouwen N, Unny TE. 1973. Flexible roughness in open channels. *J Hydr Div.* 99(5):713–728.
- Licci S, Delolme C, Marmonier P, Philippe M, Cornacchia L, Gardette V, Bouma T, Puijalon S. 2016.

- Effect of aquatic plant patches on flow and sediment characteristics: the case of *Callitriche platycarpa* and *Elodea nuttallii*. Hydrodynamic and mass transport at freshwater aquatic interfaces. Cham: Springer; p. 129–140.
- Licci S, Nepf H, Delolme C, Marmonier P, Bouma TJ, Puijalón S. 2019. The role of patch size in ecosystem engineering capacity: a case study of aquatic vegetation. *Aquat Sci.* 81(3):41.
- Liu C, Nepf H. 2016. Sediment deposition within and around a finite patch of model vegetation over a range of channel velocity. *Water Resour Res.* 52(1):600–612.
- Łoboda A, Bialik RJ, Karpiński M, Przyborowski Ł. 2018a. Seasonal changes in the biomechanical properties of *Elodea canadensis* Michx. *Aquat Bot.* 147:43–51.
- Łoboda A, Przyborowski Ł, Karpiński M, Bialik R, Nikora V. 2018b. Biomechanical properties of aquatic plants: the effect of test conditions. *Limnol Oceanogr Methods.* 16(4):222–236.
- Luhar M, Nepf HM. 2011. Flow-induced reconfiguration of buoyant and flexible aquatic vegetation. *Limnol Oceanogr.* 56(6):2003–2017.
- Marin-Diaz B, Bouma TJ, Infantes E. 2020. Role of eelgrass on bed-load transport and sediment resuspension under oscillatory flow. *Limnol Oceanogr.* 65(2):426–436.
- Marion A, Nikora V, Puijalón S, Bouma T, Koll K, Ballio F, Tait S, Zaramella M, Sukhodolov A, O'Hare M, et al. 2014. Aquatic interfaces: a hydrodynamic and ecological perspective. *Journal of Hydraulic Research.* 52(6):744–758.
- Marjoribanks TI, Hardy RJ, Lane SN, Tancock MJ. 2017. Patch-scale representation of vegetation within hydraulic models. *Earth Surf Process Landforms.* 42(5):699–710.
- Marjoribanks TI, Lague D, Hardy R, Boothroyd R, Leroux J, Mony C, Puijalón S. 2019. Flexural rigidity and shoot reconfiguration determine wake length behind saltmarsh vegetation patches. *J Geophys Res Earth Surf.* 124(8):2176–2196.
- Meire DW, Kondziolka JM, Nepf HM. 2014. Interaction between neighboring vegetation patches: impact on flow and deposition. *Water Resour Res.* 50(5):3809–3825.
- Murray A, Knaapen M, Tal M, Kirwan M. 2008. Biomorphodynamics: physical-biological feedbacks that shape landscapes. *Water Resour Res.* 44(11):1–18.
- Niklas KJ. 1992. *Plant biomechanics: an engineering approach to plant form and function.* Chicago: University of Chicago press.
- Paul M, Bouma T, Amos CL. 2012. Wave attenuation by submerged vegetation: combining the effect of organism traits and tidal current. *Mar Ecol Prog Ser.* 444:31–41.
- Przyborowski Ł, Łoboda AM, Bialik RJ, Västilä K. 2019. Flow field downstream of individual aquatic plants – experiments in a natural river with *Potamogeton crispus* L. and *Myriophyllum spicatum* L. *Hydrol Processes.* 33(9):1324–1337.
- Puijalón S, Bornette G. 2004. Morphological variation of two taxonomically distant plant species along a natural flow velocity gradient. *New Phytol.* 163(3):651–660.
- Puijalón S, Bouma TJ, Douady CJ, van Groenendaal J, Anten NP, Martel E, Bornette G. 2011. Plant resistance to mechanical stress: evidence of an avoidance-tolerance trade-off. *New Phytol.* 191(4):1141–1149.
- Puijalón S, Bouma TJ, Van Groenendaal J, Bornette G. 2008a. Clonal plasticity of aquatic plant species submitted to mechanical stress: escape versus resistance strategy. *Ann Bot.* 102(6):989–996.
- Puijalón S, Léna JP, Rivière N, Champagne JY, Rostan JC, Bornette G. 2008b. Phenotypic plasticity in response to mechanical stress: hydrodynamic performance and fitness of four aquatic plant species. *New Phytol.* 177(4):907–917.
- Rietkerk M, van de Koppel J. 2008. Regular pattern formation in real ecosystems. *Trends Ecol Evol.* 23(3):169–175.
- Rominger JT, Nepf HM. 2014. Effects of blade flexural rigidity on drag force and mass transfer rates in model blades. *Limnol Oceanogr.* 59(6):2028–2041.
- Sand-Jensen K, Mebus JR. 1996. Fine-scale patterns of water velocity within macrophyte patches in streams. *Oikos.* 76(1):169–180.
- Sand-Jensen K. 1998. Influence of submerged macrophytes on sediment composition and near-bed flow in lowland streams. *Freshwater Biol.* 39(4):663–679.
- Sand-Jensen K, Madsen TV. 1992. Patch dynamics of the stream macrophyte, *Callitriche cophocarpa*. *Freshwater Biol.* 27(2):277–282.
- Schoelynck J, Creëlle S, Buis K, De Mulder T, Emsens W-J, Hein T, Meire D, Meire P, Okruszko T, Preiner S, et al. 2018. What is a macrophyte patch? Patch identification in aquatic ecosystems and guidelines for consistent delineation. *Ecohydrol Hydrobiol.* 18(1):1–9.
- Schoelynck J, Meire D, Bal K, Buis K, Troch P, Bouma T, Meire P, Temmerman S. 2013. Submerged macrophytes avoiding a negative feedback in reaction to hydrodynamic stress. *Limnologica.* 43(5):371–380.
- Siniscalchi F, Nikora VI, Aberle J. 2012. Plant patch hydrodynamics in streams: mean flow, turbulence, and drag forces. *Water Resour Res.* 48(1):1–14.
- Sukhodolov A, Sukhodolova T, Aberle J. 2022. Modelling of flexible aquatic plants from silicone syntactic foams. *J Hydraul Res.* 60(1):173–181.
- Sukhodolova T. 2008. *Studies of turbulent flow in vegetated river reaches with implications for transport and mixing processes.* Berlin, Mathematisch-Naturwissenschaftliche Fakultät II: Humboldt-Universität zu.
- Temmerman S, Meire P, Bouma TJ, Herman PM, Ysebaert T, De Vriend HJ. 2013. Ecosystem-based coastal defence in the face of global change. *Nature.* 504(7478):79–83.
- Tinoco RO, Coco G. 2016. A laboratory study on sediment resuspension within arrays of rigid cylinders. *Adv Water Resour.* 92:1–9.
- Tschisgale S, Löhner B, Meller R, Fröhlich J. 2021. Large eddy simulation of the fluid-structure interaction in an abstracted aquatic canopy consisting of flexible blades. *J Fluid Mech.* 916:A43.
- Vandenbruwaene W, Temmerman S, Bouma TJ, Klaassen PC, de Vries MB, Callaghan DP, van Steeg P, Dekker F, van Duren LA, Martini E, et al. 2011. Flow interaction with dynamic vegetation patches: implications for biogeomorphic evolution of a tidal landscape. *J Geophys Res.* 116(F1):n/a–n/a.
- Vettori D, Nikora V. 2018. Flow-seaweed interactions: a laboratory study using blade models. *Environ Fluid Mech.* 18(3):611–636.
- Vettori D, Nikora V. 2019. Flow-seaweed interactions of *Saccharina latissima* at a blade scale: turbulence, drag force, and blade dynamics. *Aquat Sci.* 81(4):1–16.

- Vettori D, Rice SP. 2020. Implications of environmental conditions for health status and biomechanics of freshwater macrophytes in hydraulic laboratories. *J Ecohydraul.* 5(1):71–83.
- Yang J, Chung H, Nepf H. 2016. The onset of sediment transport in vegetated channels predicted by turbulent kinetic energy. *Geophys Res Lett.* 43(21):11,261–211,268.
- R Core Team. 2020. R: a language and environment for statistical computing. R Foundation for Statistical Computing, Vienna, Austria. <https://www.R-project.org/>.
- Zhang X, Nepf H. 2022. Reconfiguration of and drag on marsh plants in combined waves and current. *J Fluids Struct.* 110:103539.